

AD-A171 061

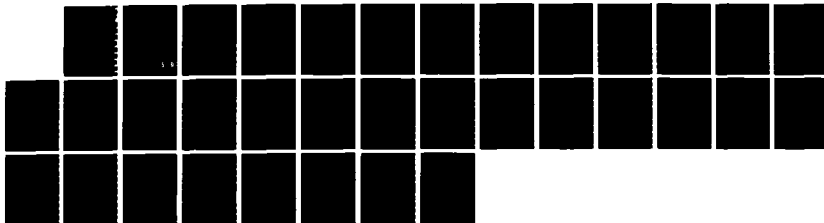
SPECTROSCOPIC STUDIES OF THE PRODUCTS OF THE REACTIONS  
OF ELECTRONICALLY. (U) PITTSBURGH UNIV PA DEPT OF  
CHEMISTRY H F GOLDE 16 JUN 86 AFOSR-TR-86-0504  
AFOSR-83-0188

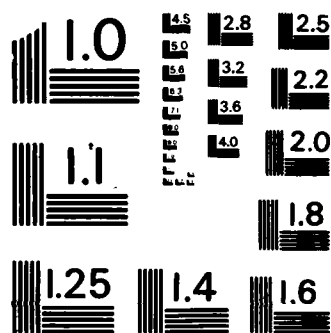
1/1

UNCLASSIFIED

F/G 7/5

NL





MICROCOPY RESOLUTION TEST CHART  
NATIONAL BUREAU OF STANDARDS-1963-A

AD-A171061

(2)

## REPORT DOCUMENTATION PAGE

1a. REPORT SECURITY CLASSIFICATION <b>Unclassified</b>			1b. RESTRICTIVE MARKINGS		
2a. SECURITY CLASSIFICATION AUTHORITY			3. DISTRIBUTION / AVAILABILITY OF REPORT Approved for public release; Distribution unlimited		
2b. DECLASSIFICATION / DOWNGRADING SCHEDULE			5. MONITORING ORGANIZATION REPORT NUMBER(S) <b>AFOSR-TR. 88-0504</b>		
4. PERFORMING ORGANIZATION REPORT NUMBER(S) <b>FQ8671-85-00800</b>			7a. NAME OF MONITORING ORGANIZATION <b>AFOSR/NC</b>		
6a. NAME OF PERFORMING ORGANIZATION <b>University of Pittsburgh</b>	6b. OFFICE SYMBOL (if applicable)	7b. ADDRESS (City, State, and ZIP Code) <b>Bldg. 410 Bolling AFB, DC 20332-6448</b>			
6c. ADDRESS (City, State, and ZIP Code) <b>Department of Chemistry, Pittsburgh, PA 15260</b>	9. PROCUREMENT INSTRUMENT IDENTIFICATION NUMBER <b>AFOSR 83-0188</b>				
8a. NAME OF FUNDING / SPONSORING ORGANIZATION <b>AFOSR</b>	8b. OFFICE SYMBOL (if applicable) <b>NC</b>	10. SOURCE OF FUNDING NUMBERS			
8c. ADDRESS (City, State, and ZIP Code) <b>Bldg. 410 Bolling AFB, DC 20332-6448</b>		PROGRAM ELEMENT NO. <b>61102F</b>	PROJECT NO. <b>2303</b>	TASK NO. <b>B1</b>	WORK UNIT ACCESSION NO.
11. TITLE (Include Security Classification) <b>Spectroscopic Studies of the Products of the Reactions of Electronically Excited AToms and Small Molecules (U)</b>					
12. PERSONAL AUTHOR(S) <b>Michael F. Golde</b>					
13a. TYPE OF REPORT <b>Final Report</b>	13b. TIME COVERED FROM <b>4/15/83</b> TO <b>4/14/86</b>	14. DATE OF REPORT (Year, Month, Day) <b>6/16/86</b>		15. PAGE COUNT <b>34</b>	
16. SUPPLEMENTARY NOTATION					
17. COSATI CODES			18. SUBJECT TERMS (Continue on reverse if necessary and identify by block number)		
FIELD	GROUP	SUB-GROUP	Energy Transfer; electronically excited noble gas atoms and nitrogen molecules; resonance fluorescence; laser-induced fluorescence.		
19. ABSTRACT (Continue on reverse if necessary and identify by block number)					
<p>The rate constants and products of the reactions of electronically-excited Ar, Kr, and Xe atoms and <math>N_2(A^3\Sigma_u)</math> and <math>CO(a^3\Pi)</math> molecules with several oxygen-, hydrogen- and chlorine-containing compounds have been determined, using emission spectroscopy, atomic resonance fluorescence and laser induced fluorescence measurements in discharge flow systems. As found previously for the excited noble gases, there is a strong correlation between the rate constants for quenching of <math>N_2(A)</math> and the availability of accessible acceptor states of the</p>					
20. DISTRIBUTION / AVAILABILITY OF ABSTRACT <input checked="" type="checkbox"/> UNCLASSIFIED/UNLIMITED <input checked="" type="checkbox"/> SAME AS RPT <input type="checkbox"/> DTIC USERS			21. ABSTRACT SECURITY CLASSIFICATION <b>Unclassified</b>		
22a. NAME OF RESPONSIBLE INDIVIDUAL <b>Dr. F. J. Wodarczyk</b>			22b. TELEPHONE (Include Area Code) <b>(202) 767-4960</b>		22c. OFFICE SYMBOL <b>NC</b>

DTIC FILE COPY

DTIC  
ELECTE  
AUG 13 1986

19. Abstract (continued)

quenching molecule, as revealed by its absorption spectrum. Consistent with this correlation, the rate constants for several inefficient quenchers are greatly enhanced in reactions with vibrationally-excited  $N_2(A)$ .

Energy transfer leading to molecular dissociation is the dominant mechanism, when energetically allowed, for most reactions of  $N_2(A)$  studied. Similar behavior is shown by both efficient and inefficient quenchers, and the results parallel the UV photochemistry of these molecules.

In contrast to  $N_2(A)$ , the isoenergetic  $CO(a^3\Pi)$  species is quenched very efficiently by  $H_2O$ ,  $CH_4$  and  $H_2$ . The reaction products have been investigated in an attempt to gain insight into this difference in behavior.

Introduction

Good progress was made in this project, AFOSR 83-0188, in achieving the goals in the original proposal. A new apparatus was built and used extensively during the last year of the project. Our resonance-fluorescence/emission apparatus remained the work-horse for this investigation. The personnel involved in the project comprised four graduate students.

The electronically-excited species studied were the lowest metastable states of Ar, Kr, Xe, N<sub>2</sub> and CO. The energies and other relevant properties are listed in Table 1. The experimental techniques used are briefly reviewed in the next section, with principal emphasis on the new discharge-flow system used for the LIF studies. The results are discussed in the following sections: Section 3: analysis of products of the reactions of Ar\*, Kr\*, Xe\* and N<sub>2</sub>(A<sup>3</sup>Σ<sub>u</sub><sup>+</sup>) with selected reagents, which has given new insight into the favored dissociation channels; Section 4: more specific information on this first study of dark channels in the reactions of N<sub>2</sub>(A), in which the contrasting behavior of efficient and inefficient quenchers is revealed clearly in the dependence of reactivity on the extent of vibration in N<sub>2</sub>(A); Section 5: an initial study of the important reactions of CO(a<sup>3</sup>Π) with H<sub>2</sub>, CH<sub>4</sub> and H<sub>2</sub>O; Section 6: the first study of vibrational excitation in the products of the dark channels of the reactions of Ar\* and Xe\*; and Section 7: a brief account of new observations on the kinetics of electronically-excited NH<sub>2</sub>( $\tilde{A}^2A_1$ ). Section 8 is a summary of the progress made in our understanding of the reactions of electronically-excited species as a result of this project.

Approved for publication and  
distribution unlimited

## Section 2. Experimental Procedures

Two discharge-flow systems have been employed in this project. The first, which uses emission spectroscopy and atomic resonance fluorescence to detect reaction products, has been described fully;<sup>1</sup> and a new apparatus, designed for laser-induced fluorescence measurements, which is shown in Fig. 1. In both systems, Ar carrier gas, with small additions of N<sub>2</sub>, Kr, or Xe as appropriate, flows through a weak dc discharge and into an observation vessel which, in the new system, is a stainless-steel block with an internal 4 cm x 4 cm square cross-section. The total pressures are in the range 0.5 to 5 Torr and the linear velocity of the gas flow as it enters the vessel is typically 3 - 5000 cm s<sup>-1</sup>. Typical metastable concentrations are 5 x 10<sup>9</sup> cm<sup>-3</sup> (for Xe\* and Kr\*) to 1 x 10<sup>11</sup> cm<sup>-3</sup> (for N<sub>2</sub>(A)). Reagent gases at concentrations in the range 1 x 10<sup>12</sup> - 4 x 10<sup>15</sup> cm<sup>-3</sup> are added either directly into the observation vessel concentrically with the main flow for product measurements (inlet A in Fig. 1), or immediately downstream of the discharge for rate constant measurements (inlet B). For the latter experiments, it is crucial to achieve rapid mixing of the flows: the simple open side-arm, shown in Fig. 1, has been found to be unsatisfactory. Because of the rapid wall loss of the metastables, an injector which protrudes into the flow cannot be used. Therefore, a new reagent inlet was designed, which comprises a wall section, 5 mm in length, containing six evenly-spaced holes of diameter 0.3 mm, through which the reagent is carried by a small Ar flow. This stainless-steel section inserts into the pyrex flow tube with rubber O-ring seals. By observing reaction flames, it has been found that complete mixing is achieved within 1 cm (0.2 ms).

LIF employs an excimer-pumped dye laser system (Lambda-Physik EMG101E, 2002). For most of this study, Sulforhodamine B dye was used in the fundamental or frequency-doubled mode. The laser pulse energy is monitored by a Gentec joule



<div data-bbox="1286 1930 1301 1932" data-label="Text"> <p>101</p> </div> <div data-bbox="1286 1934 1301 1936" data-label="Text"> <p>102</p> </div> <div data-bbox="1286 1938 1301 1940" data-label="Text"> <p>103</p> </div> <div data-bbox="1286 1942 1301 1944" data-label="Text"> <p>104</p> </div> <div data-bbox="1286 1947 1301 1949" data-label="Text"> <p>105</p> </div> <div data-bbox="1286 1951 1301 1953" data-label="Text"> <p>106</p> </div> <div data-bbox="1286 1955 1301 1957" data-label="Text"> <p>107</p> </div> <div data-bbox="1286 1957 1301 1962" data-label="Text"> <p>108</p> </div> <div data-bbox="1286 1962 1301 1966" data-label="Text"> <p>109</p> </div> <div data-bbox="1286 1966 1301 1970" data-label="Text"> <p>110</p> </div> <div data-bbox="1286 1970 1301 1974" data-label="Text"> <p>111</p> </div> <div data-bbox="1286 1974 1301 1979" data-label="Text"> <p>112</p> </div> <div data-bbox="1286 1979 1301 1983" data-label="Text"> <p>113</p> </div> <div data-bbox="1286 1983 1301 1985" data-label="Text"> <p>114</p> </div> <div data-bbox="1286 1987 1301 1989" data-label="Text"> <p>115</p> </div> <div data-bbox="1286 1991 1301 1993" data-label="Text"> <p>116</p> </div> <div data-bbox="1286 1996 1301 1998" data-label="Text"> <p>117</p> </div> <div data-bbox="1286 2000 1301 2002" data-label="Text"> <p>118</p> </div> <div data-bbox="1286 2004 1301 2006" data-label="Text"> <p>119</p> </div> <div data-bbox="1286 2008 1301 2010" data-label="Text"> <p>120</p> </div> <div data-bbox="1286 2013 1301 2015" data-label="Text"> <p>121</p> </div> <div data-bbox="1286 2017 1301 2019" data-label="Text"> <p>122</p> </div> <div data-bbox="1286 2021 1301 2023" data-label="Text"> <p>123</p> </div> <div data-bbox="1286 2025 1301 2027" data-label="Text"> <p>124</p> </div> <div data-bbox="1286 2030 1301 2032" data-label="Text"> <p>125</p> </div> <div data-bbox="1286 2034 1301 2036" data-label="Text"> <p>126</p> </div> <div data-bbox="1286 2036 1301 2040" data-label="Text"> <p>127</p> </div> <div data-bbox="1286 2040 1301 2045" data-label="Text"> <p>128</p> </div> <div data-bbox="1286 2045 1301 2049" data-label="Text"> <p>129</p> </div> <div data-bbox="1286 2049 1301 2051" data-label="Text"> <p>130</p> </div>	<div data-bbox="1305 1930 1321 1932" data-label="Text"> <p>101</p> </div> <div data-bbox="1305 1934 1321 1936" data-label="Text"> <p>102</p> </div> <div data-bbox="1305 1938 1321 1940" data-label="Text"> <p>103</p> </div> <div data-bbox="1305 1942 1321 1944" data-label="Text"> <p>104</p> </div> <div data-bbox="1305 1947 1321 1949" data-label="Text"> <p>105</p> </div> <div data-bbox="1305 1951 1321 1953" data-label="Text"> <p>106</p> </div> <div data-bbox="1305 1955 1321 1957" data-label="Text"> <p>107</p> </div> <div data-bbox="1305 1957 1321 1962" data-label="Text"> <p>108</p> </div> <div data-bbox="1305 1962 1321 1966" data-label="Text"> <p>109</p> </div> <div data-bbox="1305 1966 1321 1970" data-label="Text"> <p>110</p> </div> <div data-bbox="1305 1970 1321 1974" data-label="Text"> <p>111</p> </div> <div data-bbox="1305 1974 1321 1979" data-label="Text"> <p>112</p> </div> <div data-bbox="1305 1979 1321 1983" data-label="Text"> <p>113</p> </div> <div data-bbox="1305 1983 1321 1985" data-label="Text"> <p>114</p> </div> <div data-bbox="1305 1987 1321 1989" data-label="Text"> <p>115</p> </div> <div data-bbox="1305 1991 1321 1993" data-label="Text"> <p>116</p> </div> <div data-bbox="1305 1996 1321 1998" data-label="Text"> <p>117</p> </div> <div data-bbox="1305 2000 1321 2002" data-label="Text"> <p>118</p> </div> <div data-bbox="1305 2004 1321 2006" data-label="Text"> <p>119</p> </div> <div data-bbox="1305 2008 1321 2010" data-label="Text"> <p>120</p> </div> <div data-bbox="1305 2013 1321 2015" data-label="Text"> <p>121</p> </div> <div data-bbox="1305 2017 1321 2019" data-label="Text"> <p>122</p> </div> <div data-bbox="1305 2021 1321 2023" data-label="Text"> <p>123</p> </div> <div data-bbox="1305 2025 1321 2027" data-label="Text"> <p>124</p> </div> <div data-bbox="1305 2030 1321 2032" data-label="Text"> <p>125</p> </div> <div data-bbox="1305 2034 1321 2036" data-label="Text"> <p>126</p> </div> <div data-bbox="1305 2036 1321 2040" data-label="Text"> <p>127</p> </div> <div data-bbox="1305 2040 1321 2045" data-label="Text"> <p>128</p> </div> <div data-bbox="1305 2045 1321 2049" data-label="Text"> <p>129</p> </div> <div data-bbox="1305 2049 1321 2051" data-label="Text"> <p>130</p> </div>	<div data-bbox="1324 1930 1339 1932" data-label="Text"> <p>101</p> </div> <div data-bbox="1324 1934 1339 1936" data-label="Text"> <p>102</p> </div> <div data-bbox="1324 1938 1339 1940" data-label="Text"> <p>103</p> </div> <div data-bbox="1324 1942 1339 1944" data-label="Text"> <p>104</p> </div> <div data-bbox="1324 1947 1339 1949" data-label="Text"> <p>105</p> </div> <div data-bbox="1324 1951 1339 1953" data-label="Text"> <p>106</p> </div> <div data-bbox="1324 1955 1339 1957" data-label="Text"> <p>107</p> </div> <div data-bbox="1324 1957 1339 1962" data-label="Text"> <p>108</p> </div> <div data-bbox="1324 1962 1339 1966" data-label="Text"> <p>109</p> </div> <div data-bbox="1324 1966 1339 1970" data-label="Text"> <p>110</p> </div> <div data-bbox="1324 1970 1339 1974" data-label="Text"> <p>111</p> </div> <div data-bbox="1324 1974 1339 1979" data-label="Text"> <p>112</p> </div> <div data-bbox="1324 1979 1339 1983" data-label="Text"> <p>113</p> </div> <div data-bbox="1324 1983 1339 1985" data-label="Text"> <p>114</p> </div> <div data-bbox="1324 1987 1339 1989" data-label="Text"> <p>115</p> </div> <div data-bbox="1324 1991 1339 1993" data-label="Text"> <p>116</p> </div> <div data-bbox="1324 1996 1339 1998" data-label="Text"> <p>117</p> </div> <div data-bbox="1324 2000 1339 2002" data-label="Text"> <p>118</p> </div> <div data-bbox="1324 2004 1339 2006" data-label="Text"> <p>119</p> </div> <div data-bbox="1324 2008 1339 2010" data-label="Text"> <p>120</p> </div> <div data-bbox="1324 2013 1339 2015" data-label="Text"> <p>121</p> </div> <div data-bbox="1324 2017 1339 2019" data-label="Text"> <p>122</p> </div> <div data-bbox="1324 2021 1339 2023" data-label="Text"> <p>123</p> </div> <div data-bbox="1324 2025 1339 2027" data-label="Text"> <p>124</p> </div> <div data-bbox="1324 2030 1339 2032" data-label="Text"> <p>125</p> </div> <div data-bbox="1324 2034 1339 2036" data-label="Text"> <p>126</p> </div> <div data-bbox="1324 2036 1339 2040" data-label="Text"> <p>127</p> </div> <div data-bbox="1324 2040 1339 2045" data-label="Text"> <p>128</p> </div> <div data-bbox="1324 2045 1339 2049" data-label="Text"> <p>129</p> </div> <div data-bbox="1324 2049 1339 2051" data-label="Text"> <p>130</p> </div>	<div data-bbox="1344 1930 1359 1932" data-label="Text"> <p>101</p> </div> <div data-bbox="1344 1934 1359 1936" data-label="Text"> <p>102</p> </div> <div data-bbox="1344 1938 1359 1940" data-label="Text"> <p>103</p> </div> <div data-bbox="1344 1942 1359 1944" data-label="Text"> <p>104</p> </div> <div data-bbox="1344 1947 1359 1949" data-label="Text"> <p>105</p> </div> <div data-bbox="1344 1951 1359 1953" data-label="Text"> <p>106</p> </div> <div data-bbox="1344 1955 1359 1957" data-label="Text"> <p>107</p> </div> <div data-bbox="1344 1957 1359 1962" data-label="Text"> <p>108</p> </div> <div data-bbox="1344 1962 1359 1966" data-label="Text"> <p>109</p> </div> <div data-bbox="1344 1966 1359 1970" data-label="Text"> <p>110</p> </div> <div data-bbox="1344 1970 1359 1974" data-label="Text"> <p>111</p> </div>
---	---	---	---

meter (ED 200). The laser baffle and light collection system (see Fig. 2), including band-pass filters in front of the photomultiplier (RCA C31034), was designed to minimize detection of scattered laser radiation and background emission from the flow tube. The signal from the pmt was detected by a gated pulse-counting system (Ortec 9315/9320), which also includes a boxcar mode. Typical gate widths are 1-10  $\mu$ s in normal operation and 100 ns in the boxcar mode.

This system has allowed very sensitive and virtually background-free detection of radicals downstream of the reaction zone. Direct observation of the reaction zone has not been possible in several reactions of interest, because of large emission signals from the reaction over the same wavelength range as that of the fluorescence; these overload the photomultiplier and (at the highest levels) are detected even in gated operation. It is planned in future to gate the photomultiplier, which will alleviate the former problem, the major limitation at present.

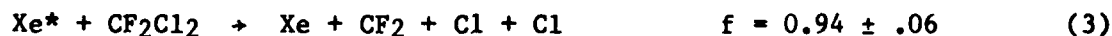
The use of the discharge-flow technique introduces much flexibility and versatility. The entire inlet assembly in each apparatus is movable, allowing the reaction zone to be positioned either in the observation zone or up to 10 cm (3 ms) upstream. An upstream observation window in the new system allows direct observation of emission from the reaction zone, while studying the reaction products downstream by LIF. The upstream inlet port (B in Fig. 1), allows addition of 'pre-reagents' to modify the distribution of metastables produced by the discharge. This was used firstly as an alternative source of  $N_2(A)$  via the reaction of  $Ar^*$  with  $N_2$ , and, secondly, for relaxation of the nascent vibrational distribution in the  $N_2(A)$  state by addition of  $CF_3H$ ,  $CF_4$  or  $CH_4$ .<sup>2</sup>

The principal results reported here are total product yields and branching fractions. In all these experiments, sufficient reagent is added to drive the

reaction rapidly to completion, allowing product analysis downstream by atomic resonance fluorescence or LIF. Branching fractions are deduced by comparison of the signals with those from reference reactions.<sup>1,3,4</sup> In a few experiments, in which nascent vibrational distributions of the products were probed, small concentrations of reagents were used. In the experiments probing the effect of vibration in  $N_2(A)$  on reaction rate constant and product distribution, a large range of reagent concentration was used, including very low values such that very little reaction occurred before the observation zone.

Section 3. Dissociation channels in the reactions of electronically excited Ar, Kr, Xe and  $N_2(A^3\Sigma^+)$ .

Previous studies<sup>1,3</sup> in the lab revealed that dark channels, involving dissociation of the reagent into non-emitting states, dominate the reactions of  $Ar^*$ ,  $Kr^*$ , and  $Xe^* np^5(n+1)s^1 3P_2$  metastable atoms, with many small molecules. Many novel reaction channels were discovered, including cleavage of more than one bond within a single collision event.



On the basis of the very large quenching rate constants and the efficient energy transfer, it was concluded<sup>4</sup> that energy transfer occurs at medium-to-long range with minimal distortion of the reagent molecule before energy transfer.

Additional evidence for this model was sought by investigating the reactions with  $NH_3$  and  $CH_3OH$  in more detail, and by extending the study to  $N_2H_4$ ,  $H_2O_2$ , and  $CH_3NH_2$ .



### 3a. Ar\* + NH<sub>3</sub>.

H-atom resonance-fluorescence measurements of the reaction of Xe\* with NH<sub>3</sub> indicated a single dominant channel



The higher-energy Ar\* metastable has additional channels available, including:



Chemionization measurements yielded a branching fraction  $f = 0.42 \pm 0.04$  for channel (5), and  $0.62 \pm 0.04$  H atoms are produced per reactive event.<sup>3</sup> These data imply an average of close to one H atom per dissociative reaction event, consistent with the occurrence of channel (6) or comparable amounts of (7) and (8). These were distinguished by measurement of the NH<sub>2</sub> yield by LIF via the NH<sub>2</sub>( $\tilde{\text{A}}^2\text{A}_1 - \tilde{\text{X}}^2\text{B}_1$ ) (090-000) band. The reference reaction was Xe\* + NH<sub>3</sub>, and the ratio [Ar\*]/[Xe\*] in the two parts of the experiment was measured directly via emission intensities from the reactions:



The total NH<sub>2</sub> yield from the Ar\* + NH<sub>3</sub> reaction was  $1.0 \pm 0.2$ . This large value is consistent with the dominance of channel (6) over (7,8), and also requires occurrence of the extremely fast secondary reaction:

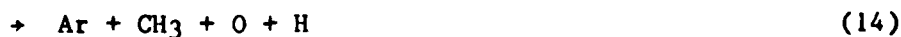


The observed weakness of the 2-atom elimination, channel (8), contrasts sharply with the results of the reactions of Ar\* with, for instance, H<sub>2</sub>O and CH<sub>4</sub>, which have similar energetics. The difference is ascribed tentatively to a symmetry effect. H<sub>2</sub>O and CH<sub>4</sub> can be excited to states of C<sub>2v</sub> symmetry with two equivalent repulsive X-H bonds, which can break simultaneously; analogous excitation of NH<sub>3</sub> yields a C<sub>3v</sub> configuration, with 3 weak bonds, so that cleavage of two bonds would require extensive rearrangement of the energy, which interestingly is not favored in this case. Curiously, a recent study of NH<sub>3</sub> photodissociation<sup>5</sup> at 121.6 nm revealed two-atom loss as the major process.



### 3b. Ar\*, Kr\*, Xe\* + CH<sub>3</sub>OH, CH<sub>3</sub>OD.

Our previous study of these reactions revealed large yields of H atoms, implying that cleavage of the C-O bond, the weakest in the molecule, is a minor process. The present study of OH LIF, using the reactions with H<sub>2</sub>O as reference, confirmed this conclusion: the branching fractions for OH production in the reactions with Xe\*, Kr\* and Ar\* are respectively < 0.03, < 0.03, and 0.13 ± 0.02 (0.15 ± 0.02 for OD from CH<sub>3</sub>OD). With these additional data, branching fractions for the allowed channels were deduced and listed in Table 2. The Ar\* reaction is of particular interest. If it is assumed that 3-atom loss, to HCO + 3H, is not important, then this reaction shows at least three separate channels, each involving cleavage of two bonds:



while cleavage of just one bond is apparently insignificant. In this reaction it is hard to envisage simultaneous cleavage of the two bonds; thus, sequential cleavage is more likely, the first dissociation releasing insufficient kinetic energy to prevent subsequent dissociation of the residual fragment.

Qualitative evidence for production of CH<sub>2</sub> in eqn. (15) was obtained in the reaction of Ar\* with CH<sub>3</sub>OD, by addition of O<sub>2</sub> downstream of the primary reaction zone. An OH signal was produced, ascribed to the reactions:



The H and D atom yields in the CH<sub>3</sub>OD reaction (1.01 and 0.46 respectively per reactive event)<sup>3</sup> are not consistent with CH<sub>2</sub>O as the sole product of channel (13). The relatively small D yield implies appreciable formation of CHOD, which may rearrange to CHDO.

The very small OH yields obtained in the reactions of CH<sub>3</sub>OH with Kr\* and Xe\* imply that the one-atom loss channels become increasingly important as the metastable energy decreases; it is thus expected that the CH<sub>3</sub>O and CH<sub>2</sub>OH are born with appreciable vibrational excitation.

### 3c. N<sub>2</sub>(A) + CH<sub>3</sub>OH, CH<sub>3</sub>NH<sub>2</sub>, N<sub>2</sub>H<sub>4</sub> and H<sub>2</sub>O<sub>2</sub>.

These reagents all have 14 valence electrons and are further related in that the central bond (C-O, C-N, N-N, O-O) is in each case the weakest bond in the molecule. The UV photochemistry of these molecules is not fully characterized, but reveals that central-bond cleavage is dominant for H<sub>2</sub>O<sub>2</sub>,<sup>6</sup> but is apparently a minor process for the other molecules.<sup>7-9</sup> Our data, summarized in Table 3, qualitatively parallel the photochemistry. Thus, the large yield of OH in the reaction with H<sub>2</sub>O<sub>2</sub> implies that the channel



has a branching fraction,  $f = 0.87 \pm 0.10$ . For  $\text{CH}_3\text{NH}_2$ , the very small  $\text{NH}_2$  yield but large H-atom yield establish cleavage of a C-H and/or an N-H bond as the major process.  $\text{CH}_3\text{OH}$  shows analogous behavior. For  $\text{N}_2\text{H}_4$ , the small  $\text{NH}_2$  yield implies a branching fraction  $f = 0.06 \pm 0.02$  for



A large H-atom resonance fluorescence signal was observed, consistent with  $\text{H} + \text{N}_2\text{H}_3$  formation, but no quantitative result was obtained, because of very rapid removal in a secondary reaction, presumably with  $\text{N}_2\text{H}_4$ .

The findings confirm our hypothesis that a long-lived intermediate, which would be expected to favor the lowest-energy channel, is not generally involved in these reactions.

Study of the reactions of  $\text{Ar}^*$  and  $\text{Xe}^*$  with  $\text{CH}_3\text{NH}_2$  and  $\text{N}_2\text{H}_4$  has also been commenced ( $\text{H}_2\text{O}$  impurity hampers study of the interesting analogous reactions of  $\text{H}_2\text{O}_2$ ). For  $\text{CH}_3\text{NH}_2$ , the yields of  $\text{NH}_2$  are uniformly low (the possible secondary reaction,  $\text{NH}_2 + \text{CH}_3\text{NH}_2$ , was shown independently to be unimportant under our conditions). For  $\text{N}_2\text{H}_4$ , the  $\text{NH}_2$  yield increased with metastable energy, as shown in Table 3.

#### Section 4. Reactions of $\text{N}_2(\text{A}^3\Sigma_u^+)$ .

When this study was commenced, limited data were available on the rate constants of the reactions of  $\text{N}_2(\text{A})$ ,<sup>10</sup> and much less was known about the reaction products. Our study has revealed that the products are consistent with those for  $\text{Ar}^*$ ,  $\text{Kr}^*$  and  $\text{Xe}^*$ , extrapolated to the lower energy, 6.2 eV of  $\text{N}_2(\text{A}, v = 0)$ . Moreover, a clear picture is emerging of the factors determining the rate constants and their dependence on vibrational quantum number,  $v$ , in  $\text{N}_2(\text{A})$ .

#### 4a. Rate constants.

The justification for the present study was the realization that quenching rate constants for  $N_2(A)$  reactions show the same correlation as those for reactions of excited Ar, Kr and Xe atoms;<sup>2</sup> namely that large quenching rate constants, close to the collision number, are found if the reagent has readily accessible energy levels (as revealed by its absorption spectrum) near or below the energy of the metastable atom. For the excited noble gases, this correlation was based largely on the unusual behavior of just two reagents,  $CF_4$  and  $CF_3H$ . However, for the lower energy  $N_2(A)$  state, a much greater variety of behavior is possible, and Table 4 includes available literature data,<sup>10</sup> showing the clear qualitative correlation between quenching rate constant and the threshold for light absorption. As yet, no quantitative correlation has been attempted, either by us or by others. Our initial measurements on other reagents further support this correlation. Thus  $N_2H_4$ ,  $CH_3NH_2$ ,  $H_2O_2$  and  $Cl_2$  have been found to be efficient quenchers, and have absorption thresholds of respectively  $>220$  nm, 245 nm, 300 nm and  $\sim 400$  nm, compared to a wavelength of 200 nm, which is the equivalent of an energy of 6.2 eV. In contrast, reaction of  $N_2(A, v = 0)$  with  $H_2O$  is very inefficient,  $k < 10^{-13} \text{ cm}^3\text{s}^{-1}$ , in agreement with its absorption threshold of about 185 nm. The chlorofluoromethanes  $CFCl_3$ ,  $CF_2Cl_2$  and  $CF_3Cl$  exhibit a progressive shift in absorption threshold, from  $\sim 230$  nm ( $\sigma = 10^{-20} \text{ cm}^2$ ) for  $CFCl_3$  to below 200 nm for  $CF_3Cl$ , and the rate constants show a parallel trend, from  $2 \times 10^{-11} \text{ cm}^3\text{s}^{-1}$  for  $CFCl_3$  to  $< 10^{-13} \text{ cm}^3\text{s}^{-1}$  for  $CF_3Cl$ . The only apparent exception to the correlation encountered so far is  $C_2H_4$ , an efficient quencher but with an absorption (singlet state) threshold of  $\sim 190$  nm. However, triplet absorption occurs between 260 and 240 nm and triplet excited states, rather than the singlets observed more readily in absorption spectra, are expected to be important in energy transfer from  $N_2(A^3\Sigma_u^+)$ .

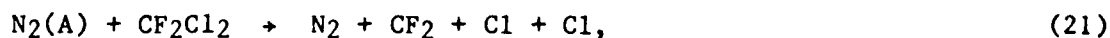
As discussed previously, we interpret the correlation as implying weak chemical forces between the excited  $N_2$  and the reagent molecule, energy transfer occurring while the reagent molecule is not significantly distorted from its equilibrium geometry.

#### 4b. Reaction Products

In addition to the reactions described in section 3, the products of the reactions of  $N_2(A)$  with  $NH_3$ ,  $O_2$ ,  $HCl$ ,  $Cl_2$ ,  $CFC1_3$ ,  $CF_2Cl_2$ ,  $CF_3Cl$ ,  $SO_2$  and  $C_2H_4$  have been investigated, using atomic O, H or Cl resonance fluorescence and emission spectroscopy. For the O- and H-containing compounds, absolute branching fractions were obtained, using the well-studied reactions of  $Ar^*$  with  $O_2$  and  $H_2$  as references.<sup>1,3</sup> No such calibration has yet been performed for the Cl-containing reagents:  $CFC1_3$  has been employed as a reference, and the following dissociation channel assumed to be dominant:



The results are summarized in Table 5 and show that dissociation is a major channel in the reactions with  $NH_3$ ,  $O_2$ ,  $HCl$ ,  $Cl_2$ ,  $CF_3Cl$  and  $CF_2Cl_2$ . Only for  $O_2$  is there evidence that other channels are important - see Section 5. The result for  $Cl_2$  contrasts with a recent study<sup>11</sup> of the reaction with IF, which yielded strong fluorescence from excited states of IF. The behavior of  $CF_2Cl_2$  and  $CF_3Cl$  is complicated by a strong dependence of the rate constant on vibrational quantum number in  $N_2(A)$ ; the values are lower limits and the very large Cl-atom yield for  $CF_2Cl_2$  suggests that a significant fraction of this reaction occurs by 2-atom loss:



thus paralleling the reaction of  $Xe^*$  with  $CF_2Cl_2$ , equ. (3).

SO<sub>2</sub> and C<sub>2</sub>H<sub>4</sub> are clear exceptions, in showing small yields of dissociation products, O and H. For SO<sub>2</sub>, this behavior contrasts with the reactions with Ar\*, Kr\*, and Xe\*, and with SO<sub>2</sub> photochemistry, which shows an onset of pre-dissociation at ~220 nm and little fluorescence at an excitation wavelength of 200 nm.<sup>6</sup> It is concluded that energy transfer from N<sub>2</sub>(A) yields non-dissociated excited states of SO<sub>2</sub>; only weak emission is observed, implying extensive quenching under the experimental conditions employed. It is likely that analogous triplet excitation is the major channel in the N<sub>2</sub>\* + C<sub>2</sub>H<sub>4</sub> reaction, analogously to the reactions of C<sub>2</sub>H<sub>4</sub> with metastable <sup>3</sup>P states of Hg, Cd and Zn.<sup>12</sup>

#### 4c. Effect of vibration in N<sub>2</sub>(A).

Vibrational relaxation within N<sub>2</sub>(A) has been studied by several groups and has been found to be very inefficient for collision partners such as the noble gases and N<sub>2</sub>. Thus, Dreyer and Perner<sup>13</sup> found relaxation by N<sub>2</sub> to have a rate constant of  $3.4 \times 10^{-16} \text{ cm}^3\text{s}^{-1}$  for N<sub>2</sub>(A, v = 1), but larger values for higher levels, ascribed to  $\Delta v = -2$  transitions. More recently, CH<sub>4</sub>, CF<sub>4</sub> and CF<sub>3</sub>H have been shown to be more efficient at vibrational relaxation,<sup>14</sup> the rate constants again increasing strongly with v. We have detected small H-atom yields when CH<sub>4</sub> is the collision partner, indicating that vibrationally-excited N<sub>2</sub>(A) undergoes weak electronic quenching in competition with vibrational relaxation but, for CF<sub>4</sub> and CF<sub>3</sub>H, electronic quenching appears to be a very minor process.

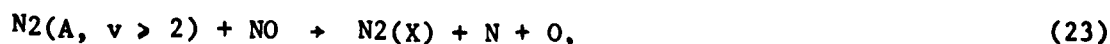
Our interest concerned, firstly, a possible v-dependence of the rate constants for electronic quenching, particularly for inefficient quenchers, and, secondly, a possible difference in quenching channels for less efficient quenchers compared to those of efficient quenchers. We have used complementary techniques: firstly, direct measurement of total quenching rate constants of N<sub>2</sub>(A, v), using emission spectroscopy, N<sub>2</sub>(A+X), or LIF, N<sub>2</sub>(B+A); secondly, the effect on the product distribution of inducing complete vibrational relaxation

in  $N_2(A)$  by the addition of  $CF_3H$  as a pre-reagent. The latter studies<sup>2</sup> are carried out firstly at very low concentrations of the principal reagent,  $Q$ , which gives information on the relative rate constants for  $v = 0$  and  $v > 0$  of the observed reaction channel; and secondly at high  $[Q]$ , which gives information on the relative branching fractions for  $v = 0$  and  $v > 0$  of the observed channel. The initial studies have been completed for  $NH_3$ ,  $CFCI_3$ ,  $O_2$ ,  $CH_3OH$  and  $NO$ ; these inspired a study of the reactions with  $H_2O$ ,  $D_2O$ ,  $CF_3Cl$ ,  $CF_2HCl$  and  $CF_2Cl_2$ , which have proved very complex and interesting and are continuing.  $NH_3$  and  $CFCI_3$  have proved to be good reference reagents: vibrational relaxation by  $CF_3H$  causes negligible changes in respectively H- and Cl-atom yields, implying that the  $v$ -dependences of rate constants and product distributions are small for these efficient quenching processes.

$CH_3OH$  shows an approximately two-fold decrease in product H-atom signal when  $CF_3H$  is added, at low concentrations of  $CH_3OH$ ; however, this effect decreases as  $[CH_3OH]$  is increased, as shown in Fig. 3. Thus, for this reagent, which quenches with a rate constant,  $k(v = 0) = 4.3 \times 10^{-12} \text{ cm}^3\text{s}^{-1}$ , the total quenching rate constant for  $v > 0$  is more than double that for  $v = 0$ , but the product distribution does not change significantly with  $v$ . Similar behavior was found for  $N_2O$ ,  $k(v = 0) = 7.7 \times 10^{-12} \text{ cm}^3\text{s}^{-1}$ , via O-atom measurements of the channel:



For  $NO$ , the product  $NO(A^2\Sigma-X^2\Pi)$   $\gamma$ -band intensity increases when  $CF_3H$  is added, the increase changing little with  $NO$  concentration. It is concluded that the rate constant for quenching does not change greatly with  $v$ , but that another channel grows in at high  $v$ . If this is ascribed to  $NO$  dissociation, endothermic for  $v < 1$ ,





then the average branching fraction for this channel is  $f_{23} = 0.22 \pm 0.03$ .

For  $O_2$ ,  $CF_3H$  reduces the O atom yield strongly at low  $[O_2]$ , and still significantly at high  $[O_2]$  (see Fig. 3). The former result is consistent with previous studies of the total quenching rate constants,<sup>15</sup> while the latter implies that the O-atom yield increases with  $v$ . Using the recent results<sup>16</sup> concerning the average branching fraction for the channel



our data imply branching fractions of 0.57 and 0.77 respectively for  $N_2(A, v = 0)$  and  $N_2(A, v > 0)$ .

These results for quenchers of intermediate efficiency have focussed attention on those of low efficiency, particularly  $H_2$ ,  $CH_4$ ,  $H_2O$ ,  $CF_3Cl$  and  $CF_2HCl$ .  $H_2$  appears to have little activity towards  $N_2(A)$  beyond very weak vibrational relaxation.  $CH_4$ , as discussed above, causes significant vibrational relaxation and much weaker electronic quenching.  $H_2O$ ,  $CF_3Cl$  and  $CF_2HCl$  show remarkable behavior: appreciable product signals (H and OH for  $H_2O$ , Cl for  $CF_3Cl$  and  $CF_2HCl$ ), which almost disappear when  $CF_3H$  is added. For none of these reagents is it possible to reach the high concentration limit at which the reaction is driven to completion (for all  $v$ ) before the observation region. The data suggest that the rate constants for the observed electronic quenching channels vary from  $k < 10^{-13} \text{ cm}^3 \text{ s}^{-1}$  for  $v = 0$  to  $k > 1 \times 10^{-11} \text{ cm}^3 \text{ s}^{-1}$  for high levels,  $v = 4-6$ . Initial studies involving direct monitoring of  $N_2(A, v)$  by LIF confirm a very large change in total deactivation rate constant. There appears to be no doubt that vibration (4 to 6 quanta, equivalent to 0.7 to 1.0 eV in energy) in  $N_2(A)$  is converting extremely inefficient electronic quenchers into rather efficient quenchers.

## Section 5. Reactions of CO(a<sup>3</sup>Π)

Although CO(a<sup>3</sup>Π) has a very similar excitation energy (6.0 eV) to that of N<sub>2</sub>(A<sup>3</sup>Σ<sub>u</sub><sup>+</sup>), its reactivity is very different; it is efficiently quenched by most reagents, including H<sub>2</sub>, CH<sub>4</sub> and H<sub>2</sub>O, which quench N<sub>2</sub>(A) extremely inefficiently.<sup>17</sup> We have thus commenced an investigation of the products of these three key reactions. In particular, we were intrigued by the possibility of an atom transfer channel:



in competition with molecular dissociation:



Results to date, however, favor channel (26) as the major and possibly the dominant process.

This study has proved difficult because the formation scheme for CO(a<sup>3</sup>Π) involves species which also quench this excited species. Several schemes have been investigated, including discharge of dilute mixtures of CO or CO<sub>2</sub> in Ar or He, and the reaction of Ar\* with CO<sub>2</sub>:



Total pressures were varied between 1 and 4 Torr. All the above schemes gave similar amounts of CO(a<sup>3</sup>Π) and most studies employed an Ar carrier, with CO<sub>2</sub> added before or after the discharge.

Two distinct experiments have been carried out. Firstly, relative H-atom resonance fluorescence signals were measured in the reactions with CH<sub>4</sub>, H<sub>2</sub>O (and NH<sub>3</sub>), using H<sub>2</sub> as the reference. The ratios obtained, I(H<sub>2</sub>)/I(RH), are listed in Table 6, and are close to two, consistent with, but not proving, the disso-

ciation mechanism, equ. (26). However, the data show significant deviations from two, suggesting at least small amounts of other quenching channels, such as (25). The relatively small H-atom yield from the  $\text{NH}_3$  reaction was surprising and is not understood as yet.

Absolute branching fractions for the reaction with  $\text{D}_2\text{O}$  (rather than  $\text{H}_2\text{O}$  to avoid interference from a small background OH signal) were sought in the second experiment:



The  $\text{D}_2\text{O}$  was added immediately downstream of the discharge (inlet B in Fig. 1), and  $\text{NO}_2$  added through the principal reagent inlet. OD was monitored in the absence and the presence of  $\text{NO}_2$ , the change in the signal being ascribed to the fast secondary reaction:



The technique was tested using the well-studied reaction  $\text{Ar}^* + \text{D}_2\text{O}$ , and gave a D/OD ratio within 20% of that expected. For  $\text{CO(a)} + \text{D}_2\text{O}$ ,  $\text{NO}_2$  addition is expected to double the OD signal if channel (28) is dominant, and to have no effect if channel (27) is dominant. The measured ratio of signals with and without  $\text{NO}_2$  was  $1.96 \pm 0.10$ .

It is thus concluded that molecular dissociation of  $\text{H}_2$ ,  $\text{CH}_4$  and  $\text{H}_2\text{O}$  is the principal channel in the reactions with  $\text{CO(a}^3\Pi)$ ; however, other channels, including reaction to  $\text{HCO}$ , may account for up to about 20% of the reaction.

#### Section 6. Vibrational distributions in the products of the reactions of $\text{Ar}^*$ and $\text{Xe}^*$ with $\text{H}_2\text{O}$ .

In the studies described so far, care was taken to ensure that the LIF measurements correctly sampled the total population of the radical,  $\text{NH}_2$  or OH.

Because of the high Ar buffer concentration,  $10^{16} - 10^{17} \text{ cm}^{-3}$ , a thermal rotational distribution was expected and confirmed by measurements on the OH(A-X)(0, 0) band. Vibrational relaxation by the carrier is less rapid but the reagents used,  $\text{H}_2\text{O}$ ,  $\text{NH}_3$ , etc., are expected to be efficient relaxers. All experiments covered a range of reagent concentration and included observations of vibrationally excited radicals, in particular OH,  $v = 1$ . It was found that vibrationally-excited OH could be relaxed completely by moderate concentrations of reagent, so that measurements of  $v = 0$  were sufficient to yield the total population.

In order to observe nascent vibrational distributions of the products, vibrational relaxation must be minimized. For  $\text{NH}_2$ , such conditions could not be achieved with the present set up, due to vibrational relaxation by Ar. For OH, relaxation by Ar is slow and nascent vibrational distributions are accessible. Initial data have been obtained for the reactions  $\text{Ar}^* + \text{H}_2\text{O}$  and  $\text{Xe}^* + \text{D}_2\text{O}$ . The reaction of  $\text{Xe}^*$  with  $\text{D}_2\text{O}$  has been studied over a ten-fold range of concentration of  $\text{D}_2\text{O}$  and with two different reaction times (movable inlet at different positions). Consistent data were obtained, yielding  $[\text{OD}(v = 1)]/[\text{OD}(v = 0)] = 0.17 \pm 0.03$ . The reaction  $\text{Ar}^* + \text{H}_2\text{O}$  could not be studied over such a wide concentration range, because background OH emission from the primary reaction interferes with the LIF measurements at low  $[\text{H}_2\text{O}]$ . The data yielded  $[\text{OH}(v = 1)]/[\text{OH}(v = 0)] \sim 0.14$ . As a check, the enhancement of OH,  $v = 0$  caused by vibrational relaxation of higher levels at higher concentrations of  $\text{H}_2\text{O}$  was measured. After correction of the LIF signals for quenching of the fluorescing  $\text{OH}(\text{A}^2\Sigma^+)$  state at these relatively high  $\text{H}_2\text{O}$  concentrations, the data yielded  $[\text{OH}(v > 0)]/[\text{OH}(v = 0)] \sim 0.20$ .

The data thus show that only a small fraction of the large amount of energy released in these reaction channels appears as vibration in the OH(OD) product.

For Xe\*, comparison can be made with measurements and calculations of photo-dissociation of H<sub>2</sub>O at comparable wavelengths,<sup>18,19</sup> which find considerably greater vibrational excitation. For Ar\*, three dissociation channels are important.



The low yield of vibration in OH(X<sup>2</sup>Π) implies that channels (32) and (33) occur by independent pathways.

### Section 7. Kinetics of electronically-excited NH<sub>2</sub>.

In using gated detection of LIF, it is important to correct for any change with conditions in the fraction of the fluorescence detected. Reagents such as H<sub>2</sub>O, NH<sub>3</sub> and N<sub>2</sub>H<sub>4</sub> are very efficient quenchers and affect the efficiency of LIF in two ways: firstly by reducing the quantum yield of fluorescence and secondly by shortening the effective lifetime of the emitting state, thus changing the fraction of fluorescence detected during the gate period. Where necessary, quenching rate constants were determined from the fluorescence decay rates as a function of reagent concentration, and corrections made. Effective electronic quenching rate constants were (cm<sup>3</sup>s<sup>-1</sup>): Ar: (4.1 ± 0.3) × 10<sup>-12</sup>; N<sub>2</sub>H<sub>4</sub>: (2.5 ± 0.3) × 10<sup>-10</sup>; NH<sub>3</sub>: (2.3 ± 0.2) × 10<sup>-10</sup>.

At low Ar pressures, the NH<sub>2</sub>\* fluorescence decays appeared to show non-exponential behavior: future experiments are planned to investigate this in more detail.

### Section 8. Summary

The products of quenching of N<sub>2</sub>(A<sup>3</sup>Σ<sub>u</sub><sup>+</sup>) and CO(a<sup>3</sup>Π) are definitely comparable to those obtained previously for the higher energy metastables Xe\*, Kr\* and Ar\*. Thus, dissociation of the reagent has been found to be the principal channel,

both for efficient and less-efficient quenchers of  $N_2(A)$ , and in the efficient reactions of  $CO(a^3\Pi)$  with  $H_2$ ,  $CH_4$ , and  $H_2O$ , which quench the isoenergetic  $N_2(A)$  very slowly. However, unlike the reactions with the excited noble gases, two reagents,  $C_2H_4$  and  $SO_2$ , have been found for which reaction with  $N_2(A)$  yields little dissociation, although it is energetically allowed.

The rapid reactions of  $N_2(A)$  with  $N_2H_4$  and  $CH_3NH_2$  do not occur significantly via cleavage of the weakest bond, confirming the non-statistical nature of the energy transfer, and the close relationship to the photochemistry of these molecules. It is thus particularly interesting that the much slower reaction,  $N_2(A) + CH_3OH$ ,  $k = 4 \times 10^{-12} \text{ cm}^3\text{s}^{-1}$ , exhibits identical behavior, showing that the mechanism of energy transfer is fundamentally unchanged, although the probability per collision is decreased, because of the reduced access to acceptor states of  $CH_3OH$ .

Despite the importance of dissociation in the unexpectedly fast reactions of  $CO(a)$  with  $H_2$ ,  $CH_4$  and  $H_2O$ , a different mechanism must be involved, as excited states of these molecules are simply not accessible without distortion of the molecule. It is thus likely that the interactions between  $CO(a)$  and these molecules are considerably more attractive than those with  $N_2(A)$ . Ab initio calculations of the  $CO(a^3\Pi) + H_2$  system have been commenced in collaboration with Professor Ken Jordan of this department, and indicate an attractive  $C_2v$  approach of the C end of CO to the  $H_2$  molecule. It is thus possible that a formaldehyde-like intermediate is involved; however, it is surprising that both H atoms are lost from this intermediate.

In comparable reactions of excited  $^3P$  states of the alkaline earth metals and of Zn and Cd with  $H_2$ , similar intermediates lead to formation of  $MH + H$  products,<sup>12,20</sup> the M-H bond energies being comparable to that of the H-CO. However, the excited metal states do not have sufficient energy to produce

$M + H + H$ . Thus, if these reactions are indeed comparable, HCO is expected to be at least a minor product, as appears to be indicated by some of the results reported in section 5.

This study has shown that many inefficient quenchers of  $N_2(A, v = 0)$  show a large increase in rate constant with  $v$ . This is wholly consistent with our model for the reactions of  $N_2(A)$ , as the increased energy improves access to excited states of these molecules. The effect is thus ascribed principally to that of energy rather than to a specific effect solely of the vibrational motion. In support of this, the rate constants for electronic quenching of  $N_2(A, v)$  by  $D_2O$  and  $CF_2HCl$  appear to increase only slightly between  $v = 0$  and 1, but more strongly between  $v = 1$  and 2.

For  $H_2$ ,  $CF_3H$ ,  $CH_4$  and  $CF_4$ , however, the lowest excited states are too high in energy to be readily accessible from  $N_2(A, v)$ , so that little electronic quenching is observed even at high  $v$ .

Table 1

Properties of the lowest metastable excited states  
of Ar, Kr, Xe, N<sub>2</sub> and CO.

Species	State	Energy, eV	Radiative Lifetime, s
Ar	$3p^5 4s^3 P_0$	11.7	45
	$3P_2$	11.5	>1.3
Kr	$4p^5 5s^3 P_2$	9.9	>1.0
Xe	$5p^5 6s^3 P_2$	8.3	~150
N <sub>2</sub>	$A^3 \Sigma_u^+$	6.2	1.3
CO	$a^3 \Pi$	6.0	$7.6 \times 10^{-3}$



Table 2

Product distributions in the reactions of Ar\*, Kr\*, Xe\* with CH<sub>3</sub>OH

Products:	Threshold Energy, eV	Branching Fractions		
		Ar*	Kr*	Xe*
CH <sub>3</sub> + OH	4.0	~0	<0.03	<0.03
CH <sub>2</sub> OH + H	4.0	~0	0.28±0.03	0.49±0.03
CH <sub>3</sub> O + H	4.5	~0		
CH <sub>2</sub> O + 2H	5.4	0.62±0.02	0.71±0.03	0.50±0.03
CH <sub>3</sub> + O + H	8.4	0.04±0.02	0±0.02	b
CH <sub>2</sub> + OH + H	8.6	0.13±0.02	<0.03	b
CHO + 3H	9.3	0 <sup>a</sup>	0 <sup>a</sup>	b
CH <sub>3</sub> OH <sup>+</sup> + e <sup>-</sup>	10.8	0.20 ± 0.01	b	b

a. Assumed value

b. Endothermic

Table 3

Product Yields in Reactions of  $N_2(A)$ ,  $Ar^*$  and  $Xe^*$  with  
some  $OH^-$  and  $NH_2$ -containing Reagents

Reaction	Product Species	Yield per reactive event
$N_2(A) + H_2O_2$	OH	$1.74 \pm 0.20$
$N_2(A) + CH_3OH$	OH	$0.01 \pm 0.01$
	H	$0.88 \pm 0.07$
$N_2(A) + CH_3NH_2$	$NH_2$	$< 0.03$
	H	$1.00 \pm 0.02$
$N_2(A) + N_2H_4$	$NH_2$	$0.12 \pm 0.03$
$Xe^* + CH_3NH_2$	$NH_2$	$< 0.03$
$Ar^* + CH_3NH_2$	$NH_2$	$< 0.05$
$Xe^* + N_2H_4$	$NH_2$	$0.22 \pm 0.04$
$Ar^* + N_2H_4$	$NH_2$	$0.45 \pm 0.10$

Table 4

Rate constants for quenching of  $N_2(A^3\Sigma_u^+)$  (energy 6.2 eV)

Reagent	Absorption nm	Threshold <sup>a</sup> eV	$k_Q(N_2(A))$ <sup>b</sup> $cm^3s^{-1}$
H <sub>2</sub>	110	11.3	$1.9 \times 10^{-15}$
CH <sub>4</sub>	144	8.6	$3.2 \times 10^{-15}$
NH <sub>3</sub>	210	5.9	$\sim 1.5 \times 10^{-10}$
H <sub>2</sub> O	185	6.7	$\sim 5 \times 10^{-14}$
H <sub>2</sub> S	270	4.6	$3.0 \times 10^{-10}$
O <sub>2</sub>	200	6.2	$(2-4) \times 10^{-12}$
CO <sub>2</sub>	170	7.3	$\sim 3 \times 10^{-14}$
N <sub>2</sub> O	210	5.9	$7.7 \times 10^{-12}$
OCS	250	5.0	$2 \times 10^{-10}$
CS <sub>2</sub>	340	3.6	$1.6 \times 10^{-10}$
SO <sub>2</sub>	400	3.1	$(3-5) \times 10^{-11}$
I <sub>2</sub>	600	2.1	$6.9 \times 10^{-12}$
HCl	200	6.2	$1.3 \times 10^{-12}$
HBr	220	5.6	$7.8 \times 10^{-11}$
HI	310	4.0	$2.8 \times 10^{-10}$
CH <sub>3</sub> Cl	200	6.2	$8.0 \times 10^{-12}$
CH <sub>3</sub> OH	200	6.2	$4.3 \times 10^{-12}$
CH <sub>3</sub> CN	216	5.7	$1.9 \times 10^{-11}$
CH <sub>3</sub> SH	280	4.4	$4.3 \times 10^{-10}$

<sup>a</sup> Ref. 6<sup>b</sup> Ref. 10

Table 5

Product Yields in Some Reactions of  $N_2(A)$ .

Reagent	Product Species	Yield per Reactive Event
$NH_3$	H	$1.07 \pm 0.10$
$C_2H_4$	H	$0.20 \pm 0.07$
$O_2$	O	$1.40 \pm 0.14^a$
$SO_2$	O	$0 \pm 0.02$
$CFCl_3$	Cl	$1.0^b$
$CF_2Cl_2$	Cl	$0.96 \pm 0.10$
$CF_3Cl$	Cl	$>0.53^c$
$Cl_2$	Cl	$1.82 \pm 0.09^a$
HCl	Cl	$1.0 \pm 0.1$

a. These values should be halved to obtain the branching fractions for dissociation.

b. Assumed value.

c. Reaction not complete at observation zone.

Table 6

Relative H - Atom Yields in the Reactions of  $\text{CO}(a^3\Pi)$  with  $\text{H}_2$ ,  $\text{CH}_4$ ,  $\text{H}_2\text{O}$  and  $\text{NH}_3$ .

Reagent	H signal ( $\text{CO}(a)+\text{RH}$ )/H signal ( $\text{CO}(a)+\text{H}_2$ )
$\text{H}_2$	1.0
$\text{CH}_4$	$0.53 \pm 0.01^a$
$\text{H}_2\text{O}$	$0.45 \pm 0.02^a$
$\text{NH}_3$	$0.41 \pm 0.02^a$

a. Uncertainty given as standard deviation of the mean.

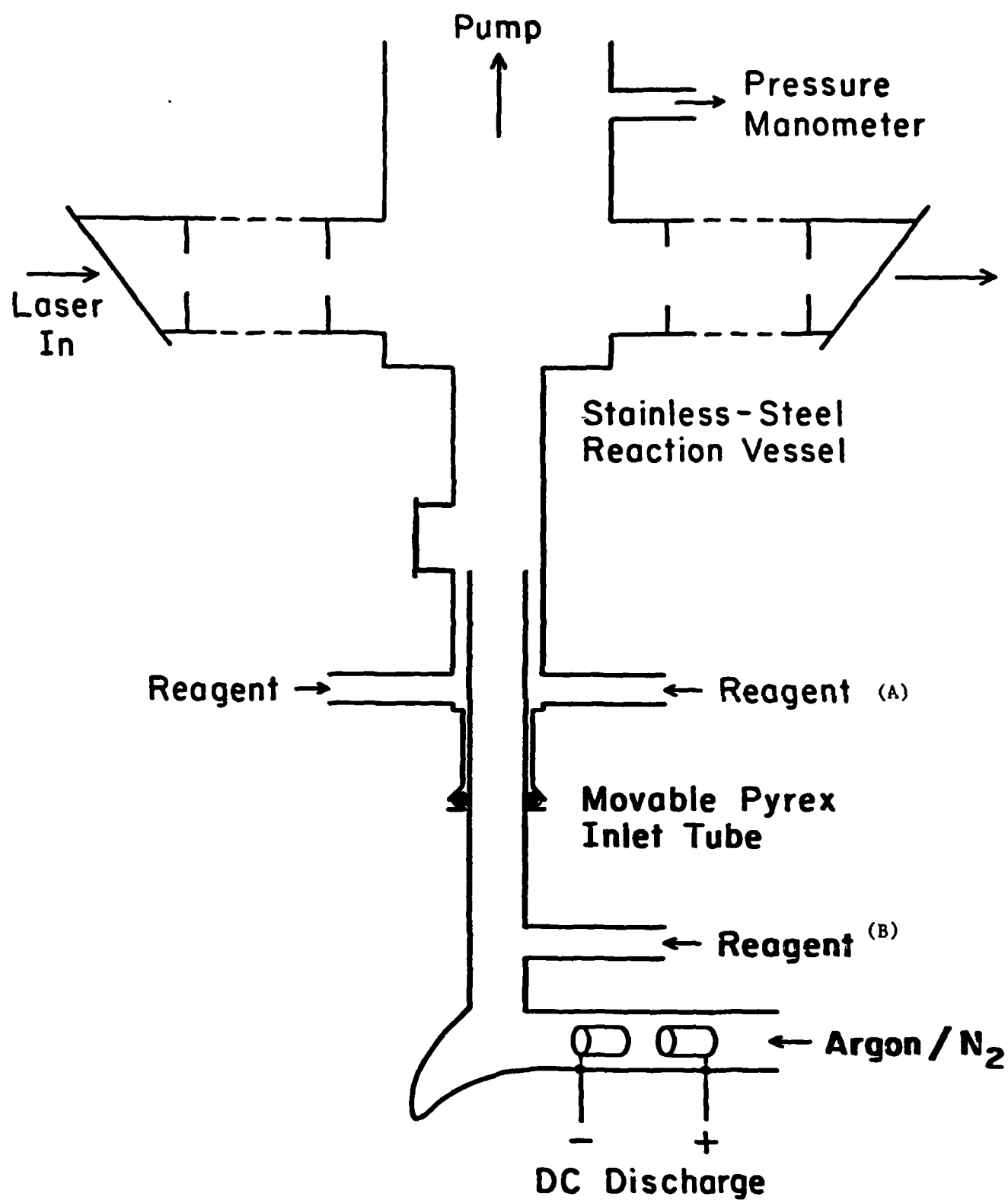


Figure 1. A schematic of the apparatus used for laser-induced fluorescence measurements.

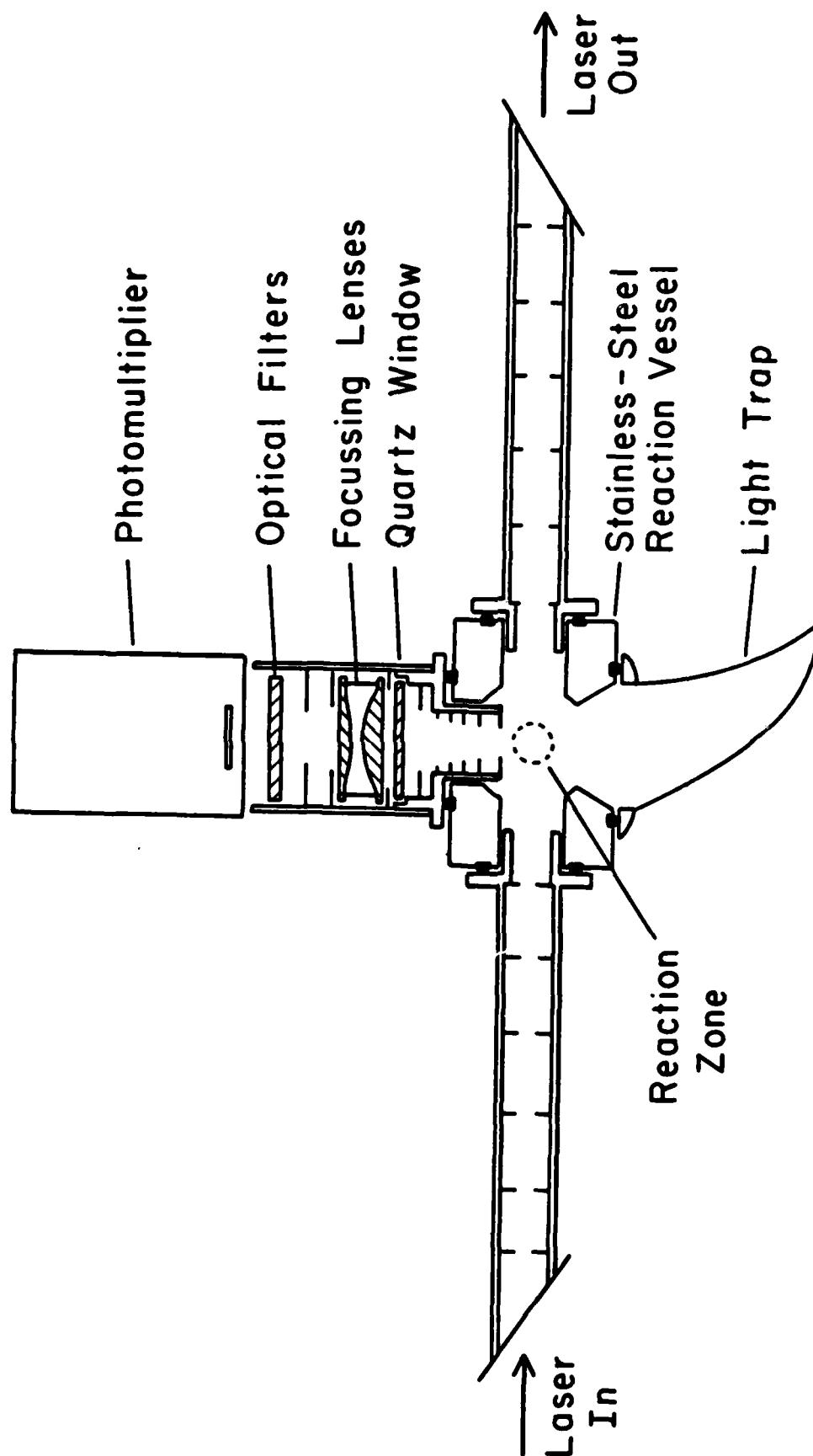


Figure 2. A cross-section through the reaction vessel showing the laser baffle and fluorescence detection systems.

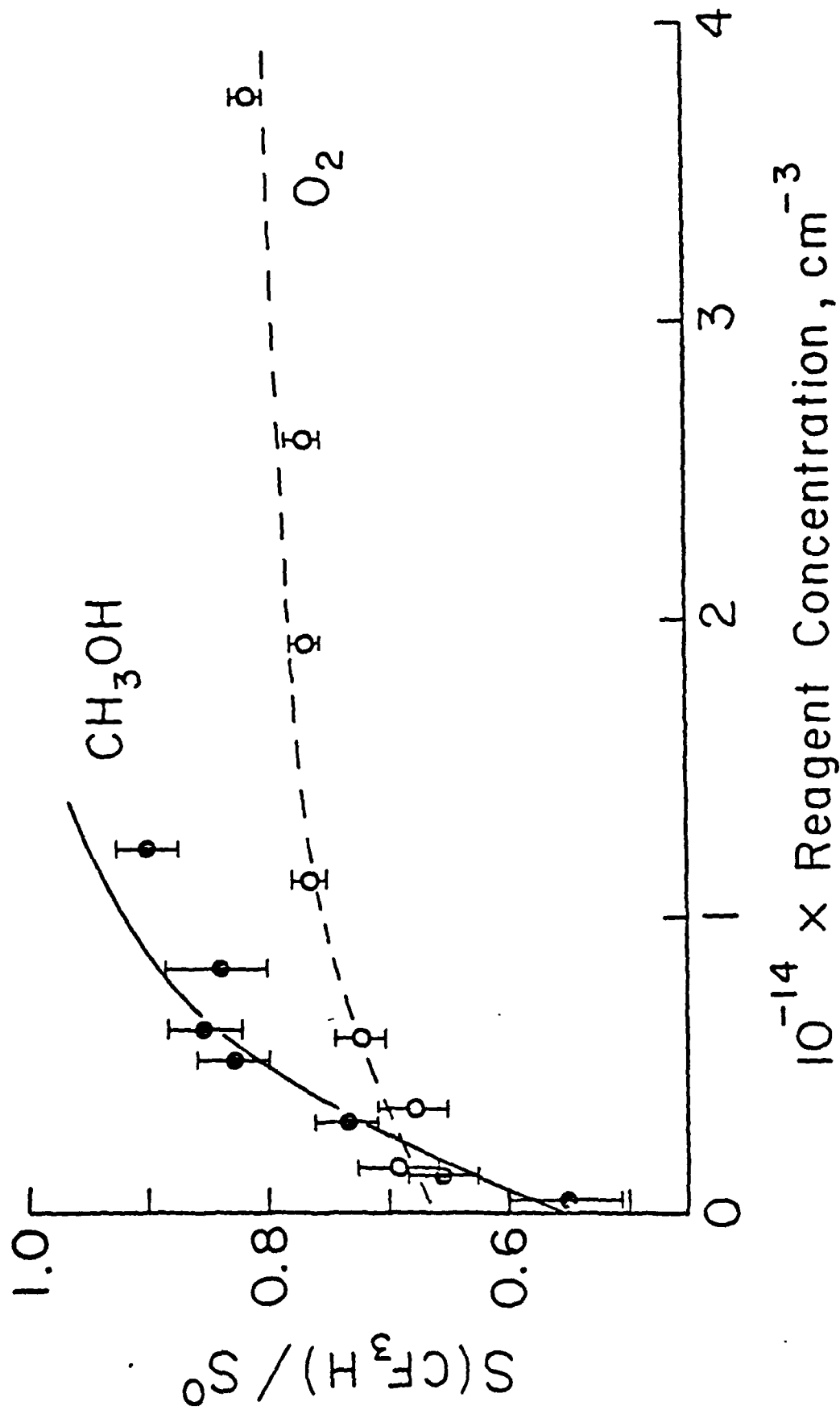


Figure 3. The effect of  $\text{CF}_3\text{H}$  addition on H- and O-atom yields in the reactions of  $\text{N}_2(\text{A})$  with respectively  $\text{CH}_3\text{OH}$  and  $\text{O}_2$ .



## References

1. J. Balamuta and M. F. Golde, J. Chem. Phys. 76 2430 (1982).
2. M. F. Golde and A. M. Moyle, Chem. Phys. Lett. 117 375 (1985).
3. J. Balamuta, M. F. Golde and Y-S. Ho, J. Chem. Phys. 79 2822 (1983).
4. J. Balamuta, M. F. Golde and A. M. Moyle, J. Chem. Phys. 82 3169 (1985).
5. T. G. Slinger and G. Black, J. Chem. Phys. 77 2432 (1982).
6. H. Okabe, Photochemistry of Small Molecules, Wiley, New York, 1978.
7. C. von Sonntag and H-P. Schuchmann, Adv. Photochem. 10 59 (1977).
8. E. P. Gardner and J. R. McNesby, J. Phys. Chem. 86 2646 (1982).
9. W. G. Hawkins and P. L. Houston, J. Phys. Chem. 86 704 (1982).
10. W. G. Clark and D. W. Setser, J. Phys. Chem. 84 2225 (1980).
11. L. G. Piper, W. J. Marinelli, W. T. Rawlins and B. D. Green, J. Chem. Phys. 83 5602 (1985).
12. W. H. Breckenridge and H. Umemoto, Adv. Chem. Phys. 50 325 (1982).
13. J. W. Dreyer and D. Perner, J. Chem. Phys. 58 1195 (1973).
14. J. M. Thomas, J. B. Jeffries and F. Kaufman, Chem. Phys. Lett. 102, 50 (1983).
15. J. M. Thomas and F. Kaufman, J. Chem. Phys. 83 2900 (1985).
16. M. P. Iannuzzi, J. B. Jeffries and F. Kaufman, Chem. Phys. Lett. 87 570 (1982).
17. K. Schofield, J. Phys. Chem. Ref. Data, 8 723 (1979).
18. P. Andresen, G. S. Ondrey, B. Titze and E. W. Rothe, J. Chem. Phys. 80 2548 (1984).
19. R. J. Buenker, G. Olbrich, H-P. Schuchmann, B. L. Schurmann and C. von Sonntag, J. Am. Chem. Soc. 106 4362 (1984).
20. W. H. Breckenridge and J-H. Wang, Chem. Phys. Lett. 123 17, 23 (1986).

**Publications: 1976 - present.**

17. R. J. Donovan, C. Fotakis and M. F. Golde, Isotope Effects in the Quenching of Electronically-Excited Atoms. Part 4. Quenching of  $I(5^2P_{1/2})$  by DCl, DBr and  $D_2O$ , JCS Faraday II, 72, 2055-63 (1976).
18. V. M. Bierbaum, M. F. Golde and F. Kaufman, Flowing Afterglow Studies of Hydronium Ion Clustering Diffusion Effects, J. Chem. Phys., 65, 2715-24 (1976).
19. M. F. Golde, Review: Reactions of Electronically Excited Noble Gas Atoms, S.P.R. 21 - "Gas Kinetics and Energy Transfer: Vol. 2, The Chemical Society, London, 1976, pp. 121-72.
20. M. P. Casassa, M. F. Golde and A. Kvaran. Emission spectra of the noble gas halides: the  $B(1/2) - A(1/2)$  system. Chem. Phys. Lett. 59, 51-6 (1978).
21. M. P. Cassassa and M. F. Golde, Vacuum UV emission by electronically excited  $N_2$ : The radiative lifetime of the  $N_2(a'^1\Sigma_u)$  state, Chem. Phys. Lett. 60 281-5 (1979).
- 22-3. M. F. Golde and A. Kvaran. Chemiluminescence of Argon Bromide.
  - I. The Emission Spectrum of ArBr.
  - II. The Potential Curves of ArBr and Population Distributions in the  $B(1/2)$  and  $C(3/2)$  Electronic States. J. Chem. Phys. 72, 434-41, 442-52 (1980).
- 24-5. M. F. Golde and R. A. Poletti. Comparison of Reactivity of  $Ar(^3P_0)$  and  $Ar(^3P_2)$  metastable states.
  - I. Rate constants for quenching by Kr and CO.
  - II. Products of quenching by some halogen-containing compounds. Chem. Phys. Lett. 80, 18-22, 23-28 (1981).
26. J. Balamuta and M. F. Golde. Quenching of metastable Ar, Kr, and Xe atoms by oxygen-containing compounds: a resonance fluorescence study of reaction products. J. Chem. Phys. 76, 2430-40 (1982).
27. M. F. Golde, Y-S. Ho and H. Ogura. Chemiluminescence reactions of metastable  $Ar(^3P_{0,2})$  atoms. J. Chem. Phys. 76, 3535-42 (1982).
28. J. Balamuta and M. F. Golde. Formation of electronically-excited oxygen atoms in the reactions of  $Ar(^3P_{0,2})$  and  $Xe(^3P_2)$  atoms with  $O_2$ . J. Phys. Chem., 86, 2765-9 (1982).
29. J. Balamuta, M. F. Golde, and Y-S. Ho. Product distributions in the reactions of excited noble-gas atoms with hydrogen-containing compounds, J. Chem. Phys. 79, 2822-30 (1983).

30. M. F. Golde and Y-S. Ho. Chemi-ionization Reactions of State-Selected Electronically-Excited  $\text{Ar}(^3\text{P}_0)$  and  $\text{Ar}(^3\text{P}_2)$  Atoms, J. Chem. Phys. 82 3160 (1985).
31. J. Balamuta, M. F. Golde and A. M. Moyle, Product Distributions in the Reactions of Excited Noble-Gas Atoms with Halogen-Containing Compounds, J. Chem. Phys. 82 3169 (1985).
32. M. F. Golde and A. M. Moyle. Reactions of Electronically-Excited  $\text{N}_2(\text{A}^3\Sigma_u^+)$ : Effect of Vibrational Excitation in  $\text{N}_2(\text{A})$ , Chem. Phys. Lett. 117 375 (1985).

**In preparation:**

33. M. F. Golde and W. Tao, Products of the Reactions of Electronically-Excited  $\text{N}_2(\text{A}^3\Sigma_u^+)$  with some OH- and  $\text{NH}_2$ -containing compounds, J. Chem. Phys.
34. M. F. Golde and G. Ho, Products of the Reactions of Electronically-Excited  $\text{CO}(\text{a}^3\Pi)$  with  $\text{H}_2$ ,  $\text{CH}_4$  and  $\text{H}_2\text{O}$ , Chem. Phys. Lett.

**Personnel**

Yueh-Se Ho: Graduate Research Student, Sept. 1980 to June 1985.  
Degree: Ph.D. Thesis: Chemiionization Reactions of Metastable Noble Gas Atoms.

Alfred M. Moyle: Graduate Research Student, Jan. 1982 to present.

Wen Tao: Graduate Research Student, Sept. 1984 to present.

Grace Ho: Graduate Research Student, Jan. 1985 to present.

**Invited Seminars**

Nov. 1985. Cornell University

Feb. 1986 Ohio State University

END

DTIC

9-86